

The bacterial effector AvrRxo1 inhibits vitamin B6 biosynthesis to promote infection in rice

Haifeng Liu^{1,2}, Chongchong Lu¹, Yang Li¹, Tao Wu¹, Baogang Zhang¹, Baoyou Liu¹, Wenjie Feng¹, Qian Xu², Hansong Dong¹, Shengyang He^{3,4,5}, Zhaohui Chu^{6,*} and Xinhua Ding^{1,*}

¹State Key Laboratory of Crop Biology, Shandong Provincial Key Laboratory for Biology of Vegetable Diseases and Insect Pests, College of Plant Protection, Shandong Agricultural University, Tai an, 271018 Shandong, PR China

²College of Agronomy, Shandong Agricultural University, Tai an, 271018 Shandong, PR China

³Department of Energy Plant Research Laboratory, Michigan State University, East Lansing, MI 48824, USA

⁴Department of Biology, Duke University, Durham, NC 27708, USA

⁵Howard Hughes Medical Institute, Duke University, Durham, NC 27708, USA

⁶State Key Laboratory of Hybrid Rice, College of Life Sciences, Wuhan University, Wuhan, 430072 Hubei, PR China

*Correspondence: Zhaohui Chu (zchu77@whu.edu.cn), Xinhua Ding (xhding@sdau.edu.cn)

<https://doi.org/10.1016/j.xplc.2022.100324>

ABSTRACT

Xanthomonas oryzae pv. *oryzicola* (*Xoc*), which causes rice bacterial leaf streak, invades leaves mainly through stomata, which are often closed as a plant immune response against pathogen invasion. How *Xoc* overcomes stomatal immunity is unclear. Here, we show that the effector protein AvrRxo1, an ATP-dependent protease, enhances *Xoc* virulence and inhibits stomatal immunity by targeting and degrading rice OsPDX1 (pyridoxal phosphate synthase), thereby reducing vitamin B6 (VB6) levels in rice. VB6 is required for the activity of aldehyde oxidase, which catalyzes the last step of abscisic acid (ABA) biosynthesis, and ABA positively regulates rice stomatal immunity against *Xoc*. Thus, we provide evidence supporting a model in which a major bacterial pathogen inhibits plant stomatal immunity by directly targeting VB6 biosynthesis and consequently inhibiting the biosynthesis of ABA in guard cells to open stomata. Moreover, AvrRxo1-mediated VB6 targeting also explains the poor nutritional quality, including low VB6 levels, of *Xoc*-infected rice grains.

Key words: rice bacterial leaf streak, effector, stomatal immunity, pyridoxal phosphate synthase, vitamin B6 (VB6), abscisic acid (ABA)

Liu H., Lu C., Li Y., Wu T., Zhang B., Liu B., Feng W., Xu Q., Dong H., He S., Chu Z., and Ding X. (2022). The bacterial effector AvrRxo1 inhibits vitamin B6 biosynthesis to promote infection in rice. *Plant Comm.* **3**, 100324.

INTRODUCTION

Rice leaf streak caused by *Xanthomonas oryzae* pv. *oryzicola* (*Xoc*) is a disease subject to international quarantine that seriously affects rice yield in tropical and subtropical areas of Asia, northern Australia, and parts of West Africa. The incidence and severity of the disease are increasing in parts of Asia where hybrid rice varieties are grown (Nino-Liu et al., 2006). *Xoc* shares high genomic DNA sequence identity with *X. oryzae* pv. *oryzae* (*Xoo*), which causes rice bacterial blight, but the two pathogens interact with rice in different manners. For example, *Xoc* invades rice leaves mainly through stomata and colonizes leaf intercellular spaces, whereas *Xoo* enters rice leaves through hydathodes and multiplies in the xylem. *Xoo* secretes transcription activator-like effectors through the type three secretion system (T3SS) to induce rice genes, including *SWEET*-family sugar transporter genes, as part of its pathogenesis mechanism (Yang et al., 2006; Chen et al., 2012). More than 40 resistance (*R*)

genes against *Xoo* have been identified in rice, whereas rice exhibits no *R* genes conferring resistance against *Xoc* strains from Asia (Zhao et al., 2005). The *Xoc* effector AvrRxo1, which is highly conserved in all tested strains of *Xoc*, was previously found to suppress nonhost resistance to *Xoo* in *Nicotiana benthamiana* (Liu et al., 2014). However, it is unclear whether AvrRxo1 plays a virulence role in its native host plant, rice, owing to the lack of an AvrRxo1-knockout mutant. AvrRxo1 also induces hypersensitive cell death in maize carrying the maize Rxo1 gene (Zhao et al., 2005) and is toxic to bacteria, yeast, and plants (Zhao et al., 2004; Liu et al., 2014; Han et al., 2015; Triplett et al., 2016). Structural analysis has shown that AvrRxo1 contains a T4 polynucleotide kinase domain and is

Published by the Plant Communications Shanghai Editorial Office in association with Cell Press, an imprint of Elsevier Inc., on behalf of CSPB and CEMPS, CAS.

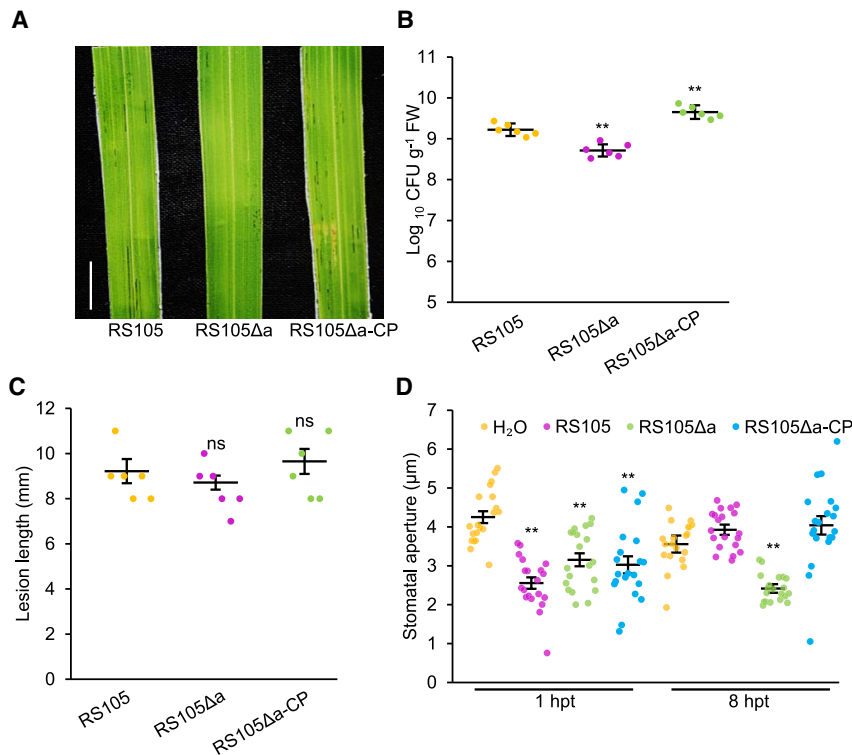


Figure 1. AvrRxo1 promotes *Xoc* infection in rice.

(A) Disease symptoms in the leaves of the wild-type rice cultivar Zhonghua11 14 days after dip inoculation (dpi) with RS105 (*Xoc* strain RS105), RS105Δa (*avrRxo1* knockout mutant), or RS105Δa-CP (complementary strain). Scale bar represents 0.5 cm.

(B) The populations of *Xoc* strains RS105, RS105Δa, and RS105Δa-CP in the leaves of wild-type Zhonghua11 rice. Bacterial growth was assessed at 14 dpi ($n = 6$; $**P \leq 0.01$; Student's *t*-test).

(C) Lesion lengths in the leaves of wild-type Zhonghua11 rice vacuum inoculated with *Xoc* strain RS105, RS105Δa, or RS105Δa-CP at 14 dpi (ns, no significance; Student's *t*-test).

(D) Stomatal apertures on the leaves of Zhonghua11 plants exposed to water or *Xoc* strain RS105, RS105Δa, or RS105Δa-CP at 1 and 8 h after inoculation ($n = 20$; $**P \leq 0.01$; Student's *t*-test).

observation suggests that AvrRxo1 is required for *Xoc* to cause disease, but its virulence contribution is most obvious when infection occurs through the leaf surface.

involved in phosphorylating nicotinamide adenine dinucleotide (NAD) to generate 3'-NADP in plants (Han et al., 2015; Schuebel et al., 2016; Triplett et al., 2016; Shidore et al., 2017). However, this does not provide a clear explanation for the role of AvrRxo1 in pathogenicity. During our study of the virulence function of AvrRxo1, we found that AvrRxo1 promotes the virulence of *Xoc* and its infection strategy by directly targeting the biosynthesis of vitamin B6 (VB6), which we found to be required for the biosynthesis of abscisic acid (ABA). The AvrRxo1-mediated inhibition of VB6 biosynthesis revealed a previously unknown step in ABA biosynthesis in plants and highlighted a novel mechanism of pathogen-mediated stomatal immunity suppression that is dependent on ABA. In addition, the effect of AvrRxo1 on VB6 biosynthesis explains the poor nutritional quality, such as low VB6 levels, of *Xoc*-infected rice grains.

RESULTS

AvrRxo1 is required for *Xoc* to reopen the stomata of rice

Although the *avrRxo1* gene was cloned in 2004 (Zhao et al., 2004), understanding of the virulence function of AvrRxo1 in the compatible *Xoc*-rice interaction is limited, partly because of the lack of an available *avrRxo1* knockout mutant. We successfully generated an *avrRxo1* knockout mutant designated RS105Δa (Supplemental Figure 1) and evaluated its virulence in Zhonghua11, a japonica-type rice cultivar that is susceptible to RS105. The RS105Δa mutant caused smaller lesions and showed lower multiplication than both wild-type RS105 and the *avrRxo1*-complementary strain when bacteria were dip inoculated onto the leaf surface (Figure 1A and 1B). However, when bacteria were infiltrated directly into the apoplast, the RS105Δa mutant showed similar multiplication to the wild-type and *avrRxo1*-complementary strains (Figure 1C and Supplemental Figure 2). This

Because *Xoc* invades unwounded rice leaves mainly through stomata, we measured the stomatal aperture of leaves dip inoculated with RS105 bacterial suspensions. At 1 h post treatment (hpt), the average stomatal aperture on inoculated leaves was significantly smaller than that on water-treated leaves (Figure 1D). At 8 hpt, the stomatal aperture of leaves inoculated with wild-type RS105 or the *avrRxo1*-complementary strain had reverted to the pre-inoculation state. Interestingly, stomatal reopening was not observed in leaves incubated with the RS105Δa mutant (Figure 1D). These results suggest that AvrRxo1 participates in stomatal reopening in rice.

AvrRxo1 targets the OsPDX1.2 protein in rice

To elucidate the molecular mechanism by which AvrRxo1 promotes *Xoc* infection in rice leaves, we performed yeast two-hybrid screening using AvrRxo1 (109–421 amino acid fragments) as bait and a rice cDNA library as prey. We screened five proteins that interacted with AvrRxo1 (Supplemental Table 3), among which OsPDX1.2 (*Os10G01080*) showed the strongest interaction (Figure 2A). OsPDX1.2 shares high sequence homology with the *Arabidopsis* pyridoxine synthase gene *AtPDX1.3* (*At5G01410*), which is associated with the production of VB6 (Titiz et al., 2006). To confirm whether full-length OsPDX1.2 and AvrRxo1 interact *in vivo*, we performed a bimolecular fluorescence complementation (BiFC) assay and a coimmunoprecipitation (coIP) assay via the transient co-expression of AvrRxo1-MYC-nYFP (N-terminal fragment of yellow fluorescent protein) and OsPDX1.2-hemagglutinin (HA)-cYFP (C-terminal fragment of yellow fluorescent protein) in the leaves of *N. benthamiana*. The yellow fluorescence signal was observed only at the border of the epidermal cells (Figure 2B), suggesting that AvrRxo1 interacts with OsPDX1.2 in plants. The coIP assay results showed that MYC-epitope-tagged AvrRxo1 was coimmunoprecipitated with HA-epitope-tagged OsPDX1.2 (Figure 2C).

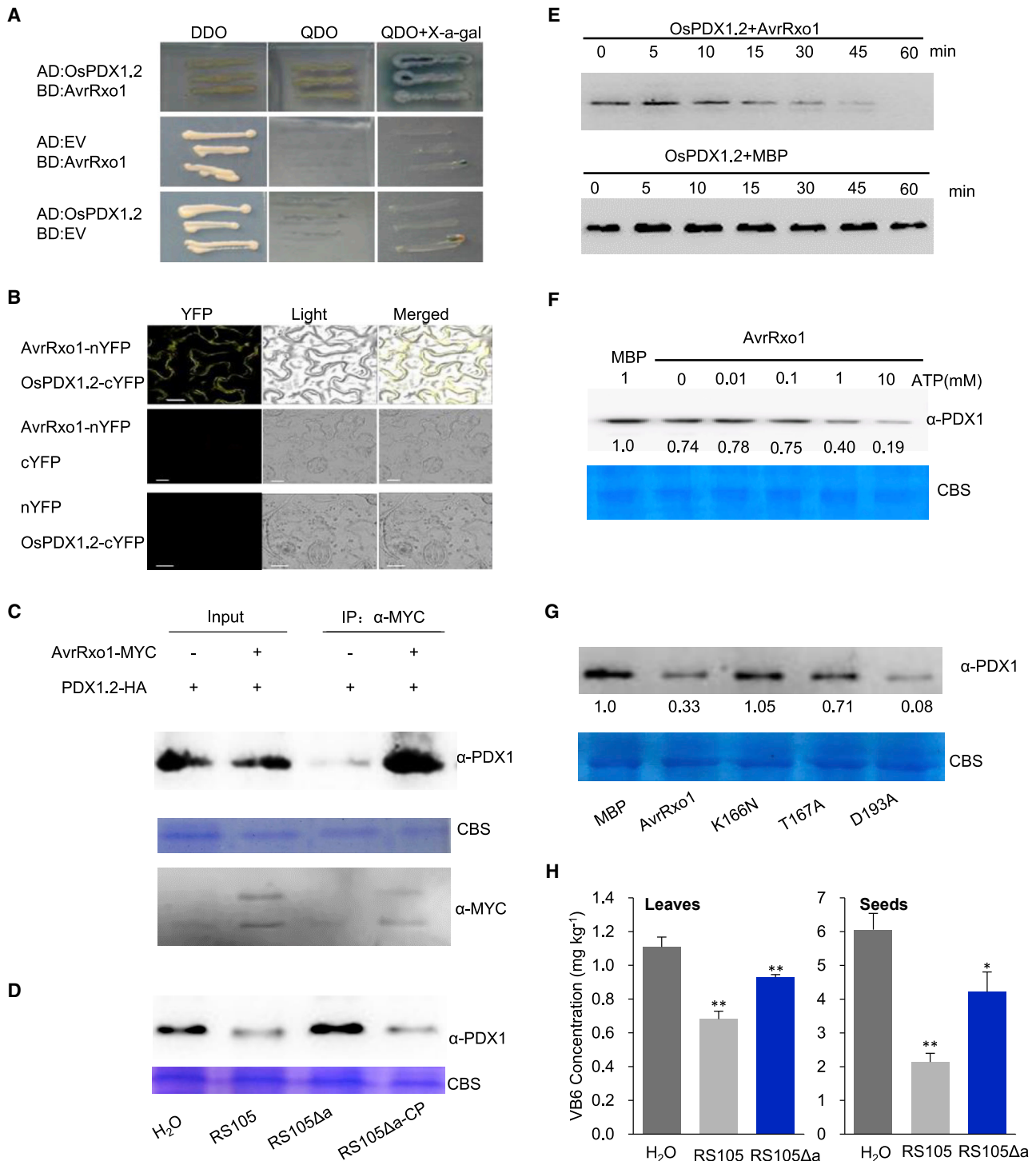


Figure 2. AvrRxo1 targets and degrades the OsPDX1.2 protein to decrease VB6 levels in rice.

(A) AvrRxo1 interacts with OsPDX1.2 in a yeast two-hybrid assay. The interaction was assessed through the growth of yeast cells on selective medium lacking Leu, Trp, His, and Ade and containing aureobasidin A and X- α -galactose (X-gal).

(B) AvrRxo1 and OsPDX1.2 interact in plants. AvrRxo1-MYC-nYFP and OsPDX1.2-HA-cYFP were transiently co-expressed in tobacco leaves, and the results were photographed 3 days later. Scale bars represent 20 μ m.

(C) AvrRxo1 interacts with OsPDX1.2 in a coIP assay. OsPDX1.2-HA and AvrRxo1-MYC or control (vector alone) were co-expressed in *N. benthamiana* leaves. coIP was carried out with an anti-MYC antibody, and the proteins were visualized by western blotting with an anti-PDX1 antibody.

(legend continued on next page)

Deletion analysis indicated that the C termini of AvrRxo1 and PDX1.2 were sufficient for the observed interaction (Supplemental Figure 3). In rice, two other PDX1 proteins, OsPDX1.1 (*Os07G01020*) and OsPDX1.3 (*Os11G48080*), share high sequence homology with OsPDX1.2 (93% and 85% identity at the amino acid level, respectively). Both OsPDX1.1 and OsPDX1.3 interact with AvrRxo1 in yeast and plant cells (Supplemental Figure 4). Because previous crystallization studies showed that PDX1 proteins from *Bacillus subtilis* form a synthase complex (Mooney et al., 2009), we analyzed the interactions among PDX1 proteins and found that PDX1 proteins from rice can assemble into homo- and heterodimers (Supplemental Figure 5). We also tested the interaction of AvrRxo1 with PDX1 proteins from the nonhost plant *Arabidopsis* and with SNZ1, a homolog involved in pyridoxine biosynthesis from yeast. All three PDX1 proteins (AtPDX1.1, AtPDX1.2, and AtPDX1.3) of *Arabidopsis* and SNZ1 of yeast interacted with AvrRxo1 (Supplemental Figure 6). Together, these data suggest that interaction with AvrRxo1 is a common feature of the PDX1 protein family that is conserved in rice (a monocot), *Arabidopsis* (a dicot), and yeast (a fungus), consistent with previous observations of the common toxic activity of AvrRxo1 in several plants and yeasts (Liu et al., 2014; Triplett et al., 2016).

AvrRxo1 targets and degrades OsPDX1.2 protein in rice

The AvrRxo1 protein is predicted to contain a protease motif (Zhao et al., 2004), which may affect the stability of PDX1 proteins. We therefore monitored the levels of the OsPDX1.2 protein in rice after *Xoc* infection. Compared with control rice plants treated with H₂O, the leaves of rice plants sprayed with RS105 or the complementary strain RS105Δa-CP showed a significantly decreased level of the OsPDX1.2 protein (Figure 2D). By contrast, rice leaves treated with RS105Δa showed a similar level of OsPDX1.2 to that observed in the H₂O-treated control. These results showed that AvrRxo1 is required for *Xoc* to decrease the level of OsPDX1.2 during infection. We also examined the levels of AtPDX1 proteins in dexamethasone-inducible, *avrRxo1*-expressing transgenic *Arabidopsis* plants (Col-0 genetic background). The dexamethasone-induced expression of AvrRxo1 resulted in a significant reduction in the AtPDX1 protein level at 24 hpt (Supplemental Figure 7).

The reduction in OsPDX1.2 and AtPDX1 levels in an AvrRxo1-dependent manner observed *in vivo* raised the possibility that AvrRxo1 may directly act as a protease on PDX1 proteins. To test this hypothesis, we performed enzyme catalysis assays using purified AvrRxo1 and OsPDX1.2 proteins and detected the degradation of OsPDX1.2 within 15 min upon AvrRxo1 addition. With increased reaction times, more OsPDX1.2 was degraded

(Figure 2E). In addition to the presence of a putative protease domain, AvrRxo1 contains a putative ATP-binding motif (Zhao et al., 2004), raising the possibility that AvrRxo1 may be an ATP-dependent protease. We therefore carried out a protein degradation assay in the presence of different concentrations of ATP. In reactions containing 1 or 10 mM ATP, OsPDX1.2 proteins were degraded by AvrRxo1, whereas in reactions containing less than 0.1 mM ATP, AvrRxo1 failed to degrade OsPDX1.2 (Figure 2F). We also generated AvrRxo1K166N and AvrRxo1T167A, which harbored mutations in the ATP-binding motif, and examined their protease activity. We found that the AvrRxo1K166N and AvrRxo1T167A mutants failed to degrade OsPDX1.2 (Figure 2G). These results indicate that ATP is required for AvrRxo1 to degrade OsPDX1.2 proteins. In addition, we examined the protease activity of the AvrRxo1D193A mutant, with a mutation at the putative kinase catalytic aspartic acid residue D193 (Han et al., 2015; Shidore et al., 2017). We observed that AvrRxo1D193A could still degrade OsPDX1.2 proteins (Figure 2G), suggesting that this putative kinase activity is not required for the protease activity of AvrRxo1. The results above reveal that AvrRxo1 targets and degrades OsPDX1.2 protein in rice infected by *Xoc*.

AvrRxo1 decreases the level of VB6 in leaves and seeds of rice

Because OsPDX1.1 and OsPDX1.2 are involved in VB6 biosynthesis in rice (Chen et al., 2014), we next investigated whether AvrRxo1 modulates the level of VB6 during *Xoc* infection by examining rice leaves inoculated with the RS105 or RS105Δa strain. Compared with plants subjected to the control (H₂O) treatment, plants inoculated with RS105 showed significantly lower VB6 levels in their leaves (Figure 2H). Interestingly, the VB6 levels of RS105Δa mutant-inoculated plants were significantly higher than those of RS105-inoculated plants but were lower than those of control-treated plants (Figure 2H), suggesting that AvrRxo1 is likely to be one of the virulence factors involved in reducing VB6 levels. We also examined the levels of VB6 in rice seeds after RS105 or RS105Δa inoculation. A lower level of VB6 was observed in the seeds of rice inoculated with RS105 than in those of the control (Figure 2H), suggesting that *Xoc* invasion could decrease the nutritional content of rice.

OsPDX1 and VB6 positively regulate rice immunity to *Xoc*

Our results obtained thus far suggested that, during *Xoc* invasion, AvrRxo1 targets OsPDX1 proteins to inhibit the synthesis of VB6. VB6 has been shown to play important roles in plant growth, development, and abiotic stress responses (Mooney et al., 2009), and it

(D) *Xoc* inoculation decreased OsPDX1.2 protein levels in rice plants. Total proteins were from wild-type Zhonghua11 inoculated with H₂O, RS105, or RS105Δa (*avrRxo1* knockout mutant) at 14 dpi. Proteins were analyzed using western blotting with an anti-OsPDX1 antibody (top panel), and overall protein loading was visualized by Coomassie blue staining (bottom panel).

(E) AvrRxo1 degrades the OsPDX1.2 protein. The AvrRxo1 and OsPDX1.2 proteins were incubated in reaction buffer for the indicated times. OsPDX1.2 proteins were visualized by western blotting with an anti-OsPDX1 antibody.

(F) ATP is required for AvrRxo1-mediated OsPDX1.2 degradation. The OsPDX1.2 and AvrRxo1 proteins were incubated in reaction buffer containing different concentrations of ATP (0–10 mM). Two hours later, OsPDX1.2 proteins were analyzed as indicated in (E).

(G) Evaluation of the ability of AvrRxo1 and the AvrRxo1K166N, AvrRxo1T167A, and AvrRxo1D193A mutants to degrade OsPDX1.2. MBP was used as a control. OsPDX1.2 proteins were analyzed as indicated in (E).

(H) The levels of VB6 in leaves or seeds of rice inoculated with H₂O, RS105, or RS105Δa (mean ± SD; n = 6; *P ≤ 0.05; **P ≤ 0.01; Student's *t*-test). The leaves were harvested at 14 dpi, and the seeds were harvested after ripening.

is required for resistance to bacterial and fungal pathogens in *Arabidopsis* and tomato (Zhang et al., 2014, 2015). To examine the role of VB6 in rice stomatal immunity against *Xoc*, a double-strand RNAi construct containing the conserved sequences of *OsPDX1.1*, *OsPDX1.2*, and *OsPDX1.3* was introduced into Zhonghua11. The transgenic lines showed significantly reduced transcript levels of *OsPDX1.1*, *OsPDX1.2*, and *OsPDX1.3*, as detected by RT-PCR (Supplemental Figure 8). When *OsPDX1*-RNAi transgenic plants were inoculated with RS105, we observed larger bacterial populations than in wild-type control plants (Figure 3A). Next, we produced transgenic rice lines overexpressing the *OsPDX1.2* gene in Zhonghua11 (Supplemental Figure 8). The transgenic lines showed greater resistance to *Xoc* than did the wild type (Figure 3B). Transgenic lines constitutively expressing the *OsPDX1.1* or *OsPDX1.3* gene also showed enhanced resistance to RS105 infection (Supplemental Figure 9). VB6 levels were 20%–30% lower in *OsPDX1*-RNAi lines and 25%–95% higher in *OsPDX1.2*-overexpressing (OE) lines (Figure 3C) than in wild-type Zhonghua11 plants. To further confirm the function of *OsPDX1.2*, two *OsPDX1.2* knockout mutants were generated via the CRISPR–Cas9 system (Supplemental Figure 10) and were observed to have lower VB6 levels (Figure 3C) and to show increased susceptibility to *Xoc* multiplication (Figure 3D). Furthermore, a decrease in the bacterial population was observed in the leaves of rice plants pretreated with VB6, suggesting that VB6 enhanced rice defense against *Xoc*. Because AvrXo1 plays a key role in defeating stomatal immunity, we further examined the stomatal apertures of *OsPDX1.2*-OE and *OsPDX1.2*-knockout (KO) lines. We observed that the average stomatal apertures were significantly smaller on *OsPDX1.2*-OE lines and significantly larger on *OsPDX1.2*-KO lines compared with the wild-type lines (Figure 3F), consistent with the positive anti-*Xoc* roles of *OsPDX1.2*. Taken together, these results suggest that *OsPDX1* and VB6 positively regulate rice stomatal immunity to *Xoc*.

VB6 is dependent on ABA biosynthesis and signaling to promote stomatal closure

ABA plays an essential role in stomatal immunity (Lim and Lee, 2015; Su et al., 2017), and the positive regulation of rice stomatal immunity to *Xoc* by VB6 encouraged us to examine the relationship between ABA and VB6. Relative to the wild type, the *OsPDX1.2*-KO mutants exhibited lower levels of ABA, whereas the *OsPDX1.2*-OE transgenic lines presented higher levels of ABA (Figure 4A and 4B), suggesting that *OsPDX1* and VB6 are associated with the ABA-metabolism-mediated regulation of rice immunity to *Xoc*.

Because the virulence function of AvrXo1 during infection is linked to stomatal reopening, we investigated whether VB6-mediated ABA metabolism may play a role in modulating stomatal immunity. To directly test this possibility, we examined the stomatal aperture in rice leaves treated with VB6. We found that VB6 treatment caused the stomata to close in both rice (Figure 4C) and *Arabidopsis* (Supplemental Figure 11). Interestingly, VB6-induced stomatal closure is dependent on ABA biosynthesis and signaling. Specifically, compared with the results observed in wild-type rice plants, stomatal responses to VB6 or ABA were greatly compromised in the leaves of the ABA-insensitive mutant *osbzip23* (Figure 4C). In *Arabidopsis*, the VB6-triggered stomatal responses of the ABA biosynthetic mutant *aba2-1* and the ABA-signaling mutant *abi1-1* were compromised (Supplemental Figure 11).

VB6 acts as a cofactor of numerous enzymes, such as those catalyzing the metabolism of amino acids and fatty acids (Mooney et al., 2009). We suspected that VB6 might promote the biosynthesis of ABA in plants. To test this hypothesis, we examined the levels of ABA in plants treated with VB6. The high-performance liquid chromatography (HPLC)–mass spectrometry (MS)/MS assay showed that the level of ABA was greatly increased after VB6 treatment (Figure 4D). VB6-activated ABA biosynthesis could also be visualized via an immunohistochemistry assay using an ABA-specific antibody. Enhanced immunofluorescence was detected in guard cells of rice leaves treated with VB6 (Figure 4E). Similarly, VB6 was found to promote ABA biosynthesis in *Arabidopsis* leaves (Supplemental Figure 12). These results strongly suggest that VB6 activates ABA biosynthesis as a mechanism to promote stomatal closure.

Because *Xoc* invasion reduces the level of VB6 (Figure 2H) and VB6 activates ABA biosynthesis (Figure 4D and 4E), we hypothesized that *Xoc* invasion leads to a reduction in ABA levels as a virulence strategy. To test this hypothesis, we quantified ABA concentrations in rice plants inoculated with the RS105, RS105 Δ a, or RS105 Δ a-complemented bacterial suspension. The results of both the HPLC–MS/MS assay (Figure 4F) and the immunohistochemistry assay (Figure 4G and Supplemental Figure 13) showed that the levels of ABA in the leaves of rice infected with RS105 or RS105 Δ a-complemented strains were significantly lower than those in H₂O-treated and RS105 Δ a-inoculated plants.

VB6 is required as a cofactor for the biosynthesis of ABA

We next investigated how VB6 promotes ABA biosynthesis. VB6 is required for the activation of molybdenum cofactor (Moco) by Moco sulfurtransferase (Seo et al., 2000a). In plants, aldehyde oxidase 3 (AO3) requires activated Moco to catalyze the oxidation of abscisic aldehyde to generate ABA (Seo et al., 2000b; Bittner et al., 2001). We therefore tested the activity of aldehyde oxidase in *OsPDX1.2*-OE transgenic plants and *OsPDX1*-KO plants by native polyacrylamide gel electrophoresis. As shown in Figure 4H, a significant decrease in AO3 activity was detected in the leaves of *OsPDX1*-KO plants, whereas in *OsPDX1.2*-OE transgenic plants, AO3 exhibited an intense band corresponding to ABA-aldehyde. We also detected a marked reduction in aldehyde oxidase activity in *Xoc*-inoculated plants (Figure 4I). Taken together, these results suggest that VB6 is required for aldehyde oxidase activity in ABA biosynthesis in plants.

ABA positively regulates rice immunity to *Xoc*

Because VB6 is required for ABA biosynthesis and positively regulates the stomatal immunity of rice against *Xoc*, we tested whether ABA affects rice defense against *Xoc*. We found that ABA treatment significantly reduced bacterial multiplication in the leaves of rice (Figure 5A). Conversely, the ABA-deficient mutant *osaba1* and the ABA-insensitive mutant *bzip23* showed significantly increased susceptibility to *Xoc* multiplication (Figure 5B and 5C). In addition, transgenic rice lines overexpressing *OsABA3* were generated and showed enhanced resistance to *Xoc* (Figure 5D). These results suggest that ABA also positively regulates rice immunity to *Xoc*.

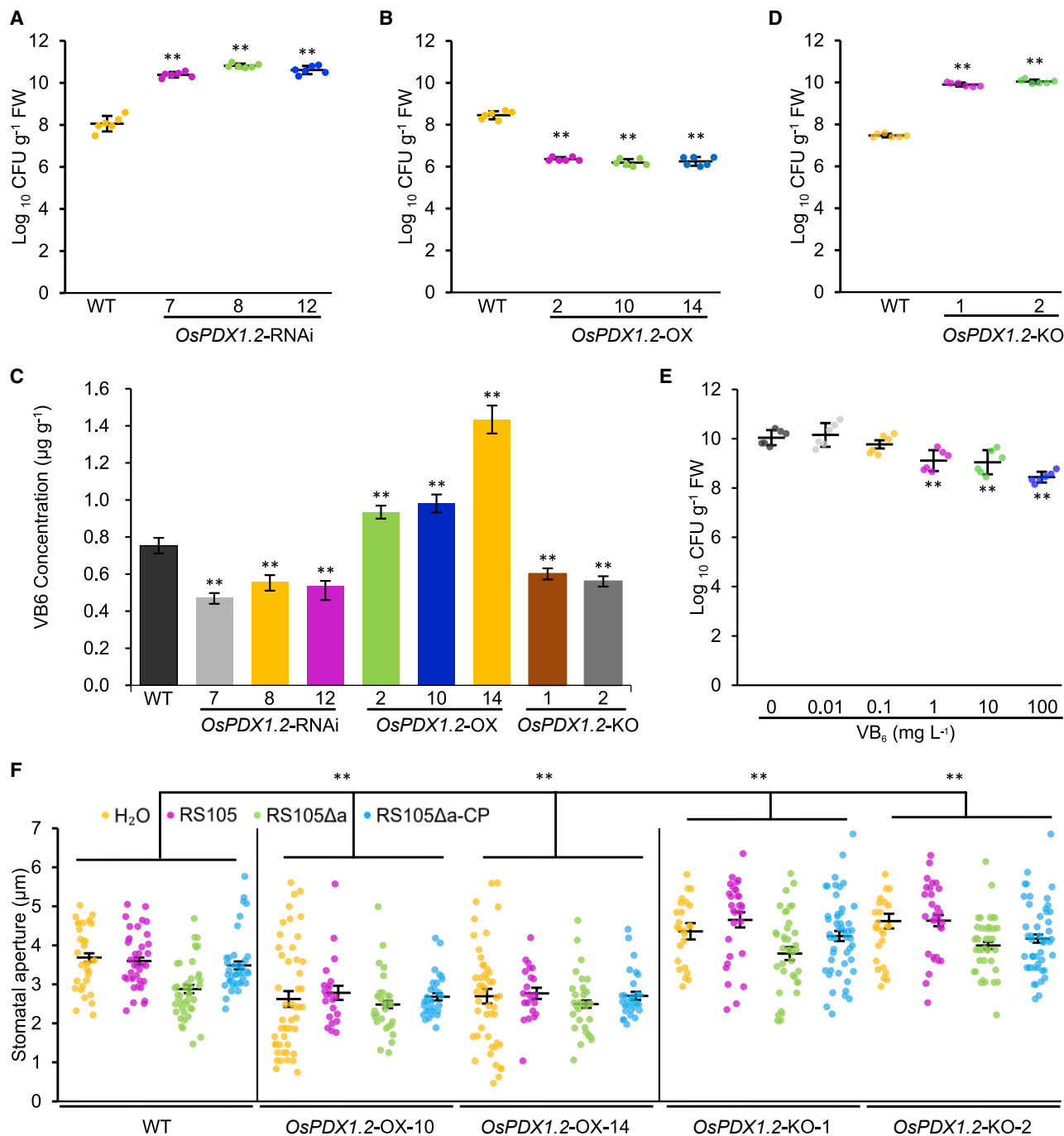


Figure 3. OsPDX1 and VB6 positively regulate rice stomatal immunity against Xoc.

(A) The populations of *Xoc* strain RS105 in the leaves of wild-type Zhonghua11 rice or *OsPDX1.2-RNAi* T1 generation transgenic plants. Bacterial growth was assessed at 14 dpi ($n \geq 6$; $**P \leq 0.01$; Student's *t*-test).

(B) The populations of *Xoc* strain RS105 in the leaves of wild-type Zhonghua11 rice or *OsPDX1.2*-overexpressing T1 generation transgenic plants. Bacterial growth was assessed at 14 dpi ($n \geq 6$; $**P \leq 0.01$; Student's *t*-test).

(C) VB6 levels in the leaves of wild-type Zhonghua11 rice, *OsPDX1.2-RNAi*, *OsPDX1.2*-overexpressing T1 generation transgenic, or *OsPDX1.2*-knockout mutant plants (mean \pm SD; $n \geq 5$; $**P \leq 0.01$; Student's *t*-test).

(D) The populations of *Xoc* strain RS105 in the leaves of wild-type Zhonghua11 rice or *OsPDX1.2*-knockout mutant plants. Bacterial growth was assessed at 14 dpi ($n \geq 6$; $**P \leq 0.01$; Student's *t*-test).

(E) VB6 enhances rice defense against *Xoc*. Populations of *Xoc* strain RS105 in the leaves of wild-type Zhonghua11 plants pretreated with the control treatment or different concentrations of VB6. Bacterial growth was assessed at 14 dpi ($n \geq 6$; $**P \leq 0.01$; Student's *t*-test).

(F) Stomatal apertures on the leaves of wild-type Zhonghua11, *OsPDX1.2*-knockout mutant plants, or *OsPDX1.2*-overexpressing transgenic plants exposed to water or *Xoc* strain RS105, RS105 Δ a, or RS105 Δ a-CP at 8 h after inoculation ($n \geq 23$; $**P \leq 0.01$; Student's *t*-test).

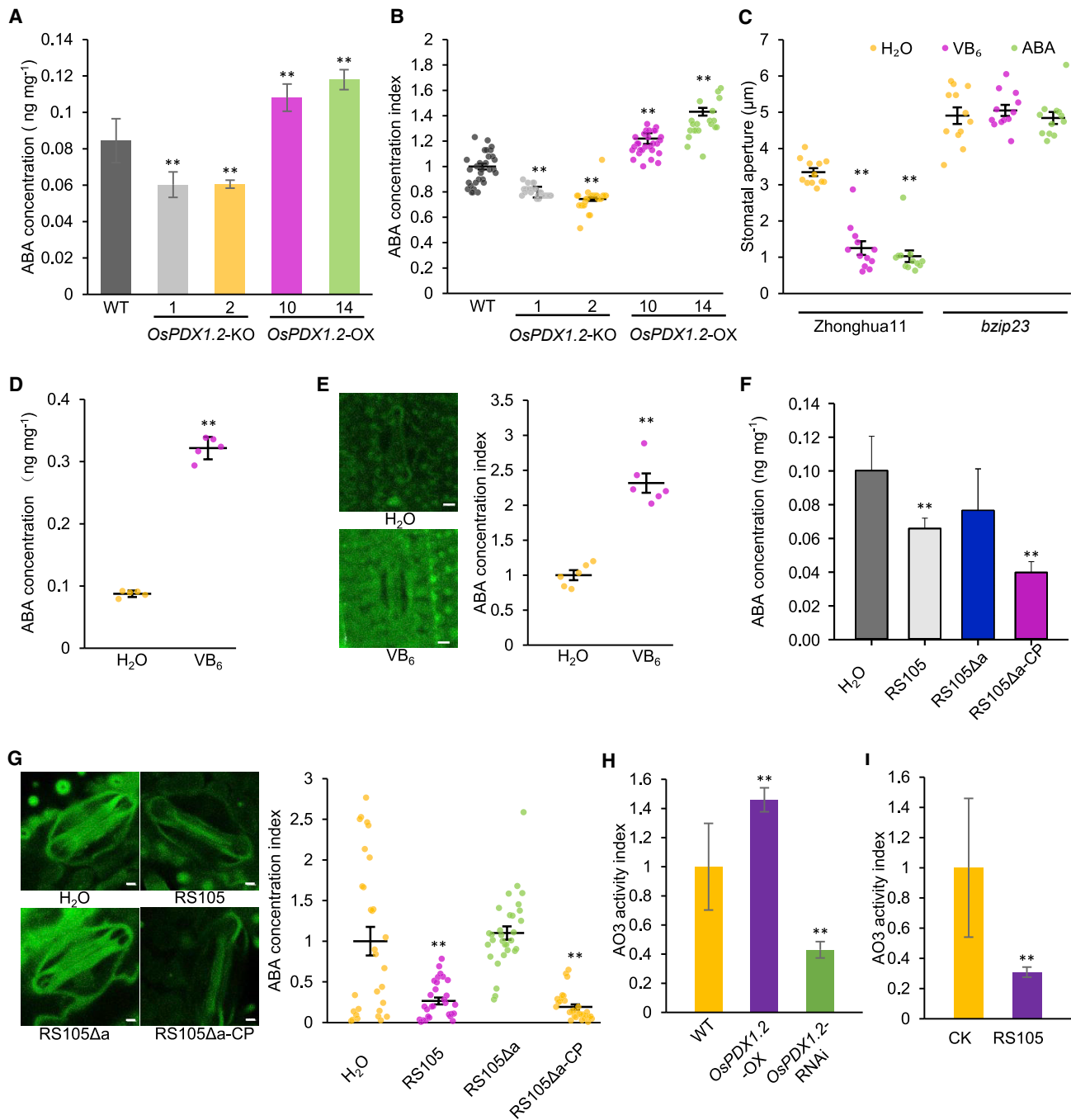


Figure 4. VB6 promotes ABA biosynthesis and stomatal closure in rice.

(A) OsPDX1.2 is associated with ABA metabolism in rice. The ABA levels in the leaves of wild-type Zhonghua11, *OsPDX1.2*-knockout mutant, or *OsPDX1.2*-overexpressing rice were measured by HPLC–MS/MS (mean ± SD; $n = 3$; $**P \leq 0.01$; Student's *t*-test).

(B) The distribution of ABA accumulation, as measured by the optimized immunofluorescence technique, in the leaves of wild-type Zhonghua11, *OsPDX1.2*-knockout mutant, or *OsPDX1.2*-overexpressing rice. The ABA/Alexa Fluor 555 fluorescence intensity analyzed by ImageJ was taken as the ABA concentration index ($n = 20$; $**P \leq 0.01$; Student's *t*-test).

(C) Stomatal apertures on the leaves of wild-type Zhonghua11 or *bzip23* (ABA-insensitive mutant) plants exposed to water, VB₆, or ABA ($n \geq 12$; $**P \leq 0.01$; Student's *t*-test).

(D) ABA levels in the leaves of wild-type Zhonghua11 plants treated with water or VB₆ ($n \geq 3$; $**P \leq 0.01$; Student's *t*-test). The leaves were harvested at 4 h posttreatment.

(E) The distribution of ABA accumulation in the leaves of wild-type Zhonghua11 ($n \geq 20$; $**P \leq 0.01$; Student's *t*-test). Leaves were harvested at 8 h after water or VB₆ treatment. Scale bars represent 1 μm. The ABA concentration index was examined as indicated in (B).

(legend continued on next page)

DISCUSSION

In this research, we found that AvrRxo1 targets and degrades OsPDX1.2, which is involved in the biosynthesis of VB6, leading to a decreased ABA level and the reopening of closed stomata (Figure 6). Previous studies showed that AvrRxo1 can phosphorylate NAD to generate 3'-NADP in bacteria, yeast, and plants (Schuebel et al., 2016; Triplett et al., 2016; Shidore et al., 2017). However, this activity could not clearly explain the virulence function of AvrRxo1 revealed in our *avrRxo1* mutant analysis. For example, reduced NAD is expected to increase ABA sensitivity (Hong et al., 2020), which conflicts with the role of ABA in regulating stomatal closure. In addition, a previous study showed that NAD kinase activity is not always associated with the toxicity of AvrRxo1 or the suppression of reactive oxygen species (ROS) by AvrRxo1 (Shidore et al., 2017). AvrRxo1-mediated NAD phosphorylation to produce 3'-NADP may play some role in AvrRxo1 toxicity, but protease activity is required for its virulence function in the context of *Xoc* infection in rice leaves, as demonstrated in this study.

ABA plays complex roles in the regulation of plant-microbe interactions (Lievens et al., 2017). As a key regulator of stomatal closure, ABA positively regulates immunity to pathogens that enter host plants mainly through the stomata, but some reports have found that ABA enhances plant susceptibility to certain pathogens (Liao et al., 2018; Zhang et al., 2019). In *Arabidopsis*, the ABA-deficient *aba3-1* mutant exhibits compromised microbe-associated molecular pattern (MAMP)- and bacterium-induced stomatal closure (Melotto et al., 2006). Similarly, *Pst* DC3000 does not induce stomatal closure in the *notabilis* tomato mutant, which lacks the ABA synthesis gene *NCED 1* (Du et al., 2014). OPEN STOMATA1 is one of the core signaling components of the ABA pathway, and the *ost1-2* mutant is defective in MAMP- and bacterium-induced stomatal closure (Melotto et al., 2006). However, some studies have shown that chitosan and the yeast elicitor YEL are able to induce stomatal closure in the *aba2-2* mutant and ABA-biosynthesis-inhibitor-treated plants (Issak et al., 2013). It has also been reported that the ABA-independent oxylipin pathway controls stomatal closure and immune defense in *Arabidopsis* (Montillet et al., 2013). In addition, a recent study demonstrated that flg22-induced stomatal closure was associated with the phosphorylation of OSCA1.3, a Ca²⁺-permeable channel that does not regulate stomatal closure upon the perception of ABA (Thor et al., 2020). These results suggest that both ABA-dependent and ABA-independent pathways play roles in stomatal defense. In this work, we found that VB6 induces stomatal closure by promoting the biosynthesis of ABA and that ABA biosynthesis and signaling are required for VB6-induced stomatal closure (Figure 4 and Supplemental Figure 11). VB6 acts as a cofactor of ABA3, which can convert

Moco from the desulfo-form into the sulfo-form. The sulfo-form of Moco is required for aldehyde oxidase AAO3 to catalyze the transformation of abscisic aldehyde to ABA (Seo et al., 2000b; Bittner et al., 2001). Thus, the AvrRxo1-mediated inhibition of VB6 biosynthesis revealed a previously unknown step in ABA biosynthesis in plants, in addition to illuminating a novel mechanism of stomatal immunity suppression by a pathogen.

In plants, stomatal closure to prevent bacteria from entering leaves has emerged as a conserved mechanism in the activation of innate immunity. Stomatal defense was first discovered while studying the *Arabidopsis*-*Pst* DC3000 interaction and was subsequently found in other plants, such as tomato and tobacco (Du et al., 2014; Murray et al., 2016). Until now, however, little has been known about whether monocots also employ stomatal defense against pathogenic bacteria. Our results show that *Xoc* invasion induces rapid stomatal closure within 1 h (Figure 1D), suggesting that stomatal defense is also involved in rice-bacteria interactions. To counteract stomatal immunity, other bacteria secrete phytotoxins or T3SS effectors to overcome stomatal defense (Melotto et al., 2017). In *Arabidopsis*, some *Pst* DC3000 effectors, such as HopF2, reduce the MAMP-triggered ROS burst to inhibit stomatal closure; other effectors, such as HopX1, HopZ1, AvrB, and the phytotoxin COR, induce jasmonic acid signaling, and the proteasome inhibitor syringolin A suppresses the salicylic acid (SA) response to inhibit stomatal defense (Schellenberg et al., 2010; Xin and He, 2013; Zheng et al., 2015; Gimenez-Ibanez et al., 2017). Recently, it was reported that the T3SS effector XopC2 of *Xoc*, as a protein kinase, phosphorylates the key component of SCFOsCOI1b to promote JAZ degradation and jasmonic acid signaling, which results in stomatal reopening (Wang et al., 2021). Here, we identified the VB6 biosynthesis gene *OsPDX1.2* as a new target of bacterial effectors to overcome stomatal defense. Notably, in addition to its presence in all *Xoc* strains, *avrRxo1* is widely conserved in other bacterial pathogens, such as *Acidovorax* and *Burkholderia*, which infect diverse plants. It remains to be determined whether AvrRxo1 targets PDX1 proteins in these plant-pathogen interactions as a widespread mechanism facilitating bacterial invasion.

PDX1 is the major gene of *de novo* VB6 biosynthesis that catalyzes more than 400 enzymes and plays an essential role in plant growth and development (Titiz et al., 2006). Because of its capacity to quench ROS, VB6 has also been found to regulate plant response to biotic and abiotic stresses. The expression of *Arabidopsis* *PDX1* genes is regulated by abiotic stresses like high light, drought, chilling, ozone, and UV radiation (Denslow et al., 2007), and the *Arabidopsis* *pdx1.3* mutant is hypersensitive to salt and UV-B treatments (Titiz et al., 2010). In

(F) ABA levels in the leaves of wild-type Zhonghua11 plants dip inoculated with RS105, RS105Δa, or RS105Δa-CP (mean ± SD; n = 3; **P ≤ 0.01; Student's *t*-test). Leaves were harvested at 14 dpi.

(G) The distribution of ABA in the leaves of wild-type Zhonghua11 plants dip inoculated with RS105, RS105Δa, or RS105Δa-CP (n ≥ 20; **P ≤ 0.01; Student's *t*-test). Leaves were harvested at 14 dpi. Scale bars represent 1 μm. The ABA concentration index was examined as indicated in (B).

(H) Aldehyde oxidase activity in the leaves of wild-type Zhonghua11, *OsPDX1.2*-overexpressing transgenic plants, or *OsPDX1*-suppressing transgenic plants. Protein extracts were subjected to native PAGE, and abscisic aldehyde was used as the substrate. The native polyacrylamide gel electrophoresis band intensity analyzed by ImageJ was taken as the aldehyde oxidase 3 (AO3) activity index (n = 3; **P ≤ 0.01; Student's *t*-test).

(I) *Xoc* infection inhibits aldehyde oxidase activity in the leaves of wild-type Zhonghua11. Leaves of Zhonghua11 plants were dipped into a bacterial suspension (1 × 10⁸ CFU/ml) of *Xoc* strain RS105. The leaves were harvested at 14 dpi (n = 3; **P ≤ 0.01; Student's *t*-test). Aldehyde oxidase activity was examined as indicated in (H).

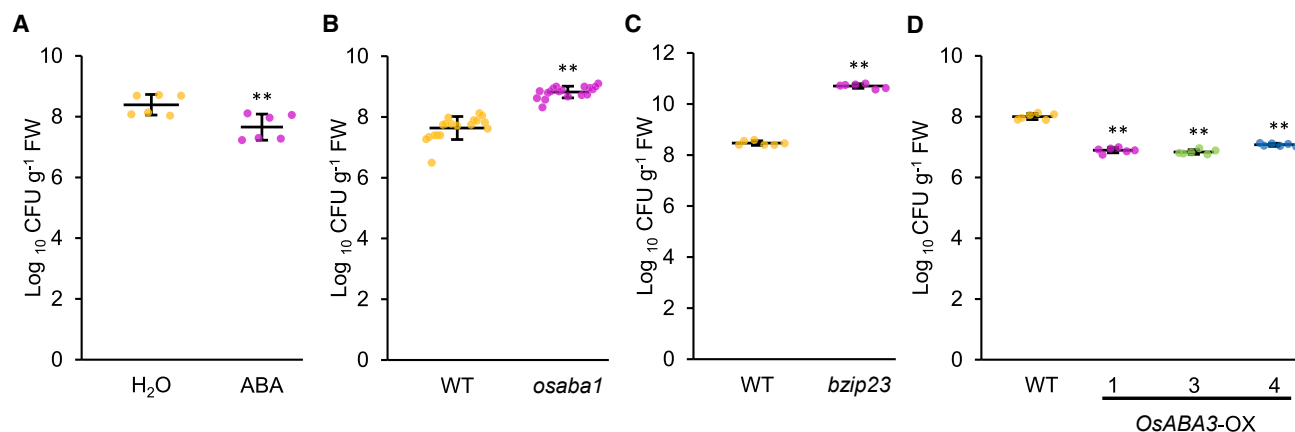


Figure 5. ABA positively regulates rice immunity to *Xoc*.

(A) ABA enhances rice defense against *Xoc*. The populations of *Xoc* strain RS105 in the leaves of wild-type Zhonghua11 plants pretreated with the control treatment or ABA (1 μM) are shown. Bacterial growth was assessed at 14 dpi (n ≥ 6; **P ≤ 0.01; Student's *t*-test).

(B) The rice *osaba1* mutant is more susceptible to *Xoc*. The populations of *Xoc* strain RS105 in the leaves of wild-type Nipponbare rice or *osaba1* mutant plants were assessed at 14 dpi (n = 18; **P ≤ 0.01; Student's *t*-test).

(C) The ABA-insensitive mutant *bzip23* is more susceptible to *Xoc*. The populations of *Xoc* strain RS105 in the leaves of wild-type Zhonghua11 rice or *bzip23* mutant plants were assessed at 14 dpi (n ≥ 6; **P ≤ 0.01; Student's *t*-test).

(D) *OsABA3*-overexpressing T1 generation transgenic plants were more resistant to *Xoc*. The populations of *Xoc* strain RS105 in the leaves of wild-type Zhonghua11 rice or *OsABA3*-overexpressing plants were assessed at 14 dpi (n = 6; **P ≤ 0.01; Student's *t*-test).

another study of its ROS quenching capacity, excess VB6 inhibited hypersensitive cell death and delayed the defense response to an ROS-dependent pathogen in tobacco (Denslow et al., 2005). It is noteworthy that the *pdx3* and *sos4* mutants, which are involved in the VB6 salvage pathway, showed higher levels of VB6 and hypersensitivity to salt stress (Titiz et al., 2006; Colinas et al., 2016). Especially in the *pdx3* mutant, there is an increased level of SA and upregulated expression of defense genes, suggesting that VB6 may act as a cofactor during SA synthesis in plants. Further studies are needed to clarify the association between VB6 and SA synthesis.

METHODS

Bacterial strains and plasmid construction

The bacterial strains and plasmids used in this study are described in Supplemental Table 1. The *Escherichia coli* strains were cultured on Luria-Bertani medium at 37°C. The *Xoc* RS105 strain was cultured on nutrient agar (NA) medium containing 50 μg ml⁻¹ rifampicin at 28°C. The *Pseudomonas syringae* pv. *tomato* strain DC3000 was cultured on King's B medium containing 50 μg ml⁻¹ rifampicin at 28°C. The *Agrobacterium tumefaciens* strains were cultured on Luria-Bertani medium containing 50 μg ml⁻¹ rifampicin at 28°C.

To generate the *avrRxo1* KO mutant, a 430-bp fragment located 88–517 bp downstream of the ATG start codon was amplified using the primers *avrRxo1*KO-F and *avrRxo1*KO-R. The fragment was inserted into the pEASY-T1 vector (TransGen, China), the construct was transformed into RS105 by electrotransformation, and the strain was cultured on NA medium containing 50 μg ml⁻¹ rifampicin and 50 μg ml⁻¹ kanamycin at 28°C.

To generate pHM1-*avrRxo1*, the *avrRxo1* gene with its promoter was amplified using the primers *AvrRxo1*-ORF1-F and *AvrRxo1*-ORF2-R, which contained *Sac* I sequences at both the 5' and 3' ends, followed by *Sac* I digestion and ligation into the pHM1 vector (Yang et al., 2006). pHM1-*avrRxo1* was transformed into RS105Δa (*avrRxo1* KO mutant) by electrotransformation and cultured on NA medium containing 50 μg ml⁻¹ rifampicin, 50 μg ml⁻¹ spectinomycin, and 50 μg ml⁻¹ kanamycin at 28°C.

In a yeast two-hybrid system, *avrRxo1*(109–421), *avrRxo1*(160–421), *avrRxo1*(164–421), *avrRxo1*(194–421), *avrRxo1*(230–421), *avrRxo1*(309–421), *avrRxo1*(364–421), *avrRxo1*(1–411), *OsPDX1.1*, *OsPDX1.3*, *OsPDX1.2*(1–313), *OsPDX1.2*(157–313), *OsPDX1.2*(184–313), *OsPDX1.2*(199–313), *OsPDX1.2*(246–313), *OsPDX1.2*(1–283), *OsPDX1.2*(1–273), *OsPDX1.2*(1–263), and *OsPDX1.2*(1–253) were amplified using the primers containing *Nco* I and *Bam*HI sites listed in Supplemental Table 2 and inserted into the pGBKT7 or pGADT7 (Clontech) vector. The plasmids were transformed into Y2H Gold cells and plated on double dropout medium (SD-Leu/-Trp) and quadruple dropout medium (SD-His/-Leu/-Trp/-Ura) (Clontech).

For BiFC and colP assays, the *AvrRxo1* and *OsPDX1.2* genes were amplified by PCR using primers containing *Bam*HI and *Hind*III sites, and the products were cloned into the pSPYNE and pSPYCE vectors (Walter et al., 2004), respectively. *OsPDX1.1*-cYFP and *OsPDX1.3*-cYFP were generated using a similar method. The primers used to amplify *avrRxo1*, *OsPDX1.1*, *OsPDX1.2*, and *OsPDX1.3* are described in Supplemental Table 2.

AvrRxo1 fused with MBP and 6×His tag was used for *Escherichia coli* fusion protein isolation. The *AvrRxo1* gene was amplified using primers containing *Bam*HI at the 5' end and *Hind*III at the 3' end, followed by *Bam*HI and *Hind*III digestion and ligation into the pMal-c2x vector (NEB). The *AvrRxo1* point mutants *AvrRxo1*^{K166N}, *AvrRxo1*^{T167A}, and *AvrRxo1*^{D193A} were generated by site-directed mutagenesis with the primers listed in Supplemental Table 2 using the pMal-c2x-*AvrRxo1* construct as the template. The *OsPDX1.2* gene was cloned into the pDONR201 entry vector via the BP reaction and then subcloned into the pET-DEST42 vector (Invitrogen). These constructs were transformed into *E. coli* strain BL-21 by electrotransformation.

The plasmids P_{ubi}:*OsPDX1.1*, P_{ubi}:*OsPDX1.2*, P_{ubi}:*OsPDX1.3*, and P_{ubi}:*OsABA3* were constructed by introducing the full-length *OsPDX1.1*, *OsPDX1.2*, *OsPDX1.3*, and *OsABA3* sequences into the *Xcm* I-digested plasmid pCXUN-HA (Chen et al., 2009). cDNA from Zhonghua11 was used as a template to amplify these fragments.

To silence *OsPDX1.2* in rice, a 263-bp fragment located at the 3' end of the *OsPDX1.2* gene was amplified using Zhonghua11 genomic DNA as a

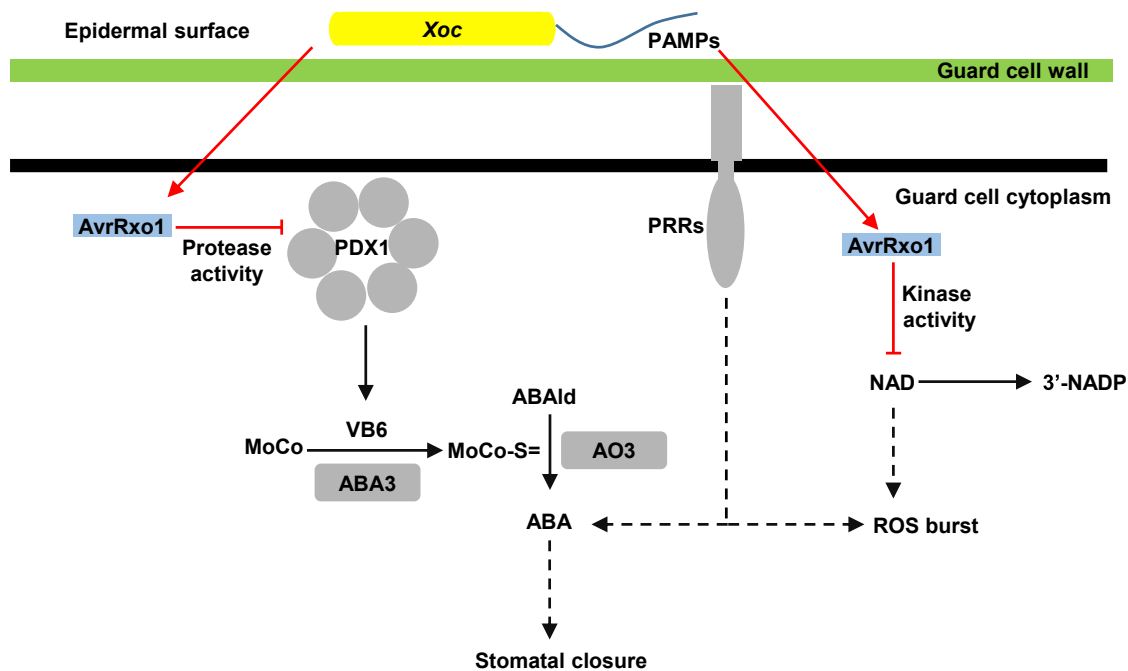


Figure 6. A model describing how AvrRxo1 targets and degrades PDX1 to inhibit vitamin B6 biosynthesis, leading to a decreased ABA level and stomatal reopening in rice.

The red and black lines indicate bacterial activity and rice enzyme activity, respectively. Arrows and T lines indicate promotion and inhibition effects, and solid and dotted lines indicate direct and indirect actions.

template, and the PCR products were digested with *Kpn I/BamH I* and inserted into the plasmid pDS1301 to obtain pDS1301-OsPDX1.2. Then, the pDS1301-OsPDX1.2 and OsPDX1.2 fragments were digested with *Sac I/Spe I* and incubated with T4 DNA ligase (NEB) to obtain OsPDX1.2-RNAi.

A CRISPR-Cas9 system obtained from Yaoguang Liu was used to knock out OsPDX1.2. The plasmids used for this purpose were constructed as described previously (Ma et al., 2016). The target sequence was 5'-GTCATGGCCAAGGCCCGCAT-3', which is located 286–305 bp downstream of the ATG start codon. All plasmids were validated by sequencing.

Plant material and growth conditions

Rice (*Oryza sativa japonica*) plants of the wild-type Zhonghua11 and Nipponbare; the *bzip23* (Zhonghua11 background; Xiang et al., 2008), *osaba1* (Nipponbare background), and *OsPDX1.2*-KO mutants; and the *OsPDX1.2*-OX, *OsPDX1.2*-RNAi, and *OsABA3*-OX transgenic lines were grown in soil in a growth house with 12-h days (at 28°C and 60%–75% relative humidity) and 12-h nights (at 24°C and 60%–75% relative humidity).

Arabidopsis thaliana wild-type Col-0, Ler, *aba2-1* (Schwartz et al., 1997), *abi1-1* (Leung et al., 1994), and transgenic lines containing DEX:*avrRxo1* were grown in nutrient substrates in an incubator with 12-h days (at 22°C and 60%–75% relative humidity) and 12-h nights (at 20°C and 60%–75% relative humidity).

N. benthamiana plants were grown in a greenhouse with 12-h days (at 22°C and 60%–75% relative humidity) and 12-h nights (at 20°C and 60%–75% relative humidity).

Rice and *Arabidopsis* transformation

Transgenic rice plants were constructed via *Agrobacterium*-mediated transformation according to published protocols (Lin and Zhang, 2005).

Agrobacterium-mediated *Arabidopsis* transformation was performed by floral dipping as described previously (Clough and Bent, 1998).

The OsPDX1 KO mutants OsPDX1.2-KO1 and OsPDX1.2-KO2 were generated using the CRISPR-Cas9 system (Ma et al., 2016). The primers used to sequence the target OsPDX1 are listed in Supplemental Table 2.

Chemical treatments

To study the effects of VB6 or ABA on disease development, VB6 (Sigma-Aldrich) or ABA (Sigma-Aldrich) solubilized in deionized H₂O supplemented with 0.05% (vol/vol) Tween 20 or ddH₂O (as a control) was sprayed on rice plants, and 4 h later, the rice plants were sprayed with bacterial suspensions (10⁸ colony-forming units [CFU] ml⁻¹). The plants were sprayed with VB6, ABA, or ddH₂O again at 4 and 8 days after inoculation. Bacterial growth was measured at 14 days after inoculation.

Xoc infection and bacterial growth assay

To evaluate bacterial leaf streak disease, 4-week-old rice plants were inoculated with bacterial suspensions (10⁸ CFU ml⁻¹) by spray or infiltration. For the spray assay, the rice was completely sprayed with the bacterial suspension in buffer containing 10 mM MgCl₂ supplemented with 0.05% (v/v) Tween 20. For the infiltration assay, the bacterial suspension in buffer containing 10 mM MgCl₂ was infiltrated into rice leaves with a needleless syringe. Bacterial growth was measured at 14 days after inoculation.

To analyze the effects of Xoc infection on the VB6 level in seeds, rice plants at the bolting stage were completely sprayed with bacterial suspension in buffer containing 10 mM MgCl₂ supplemented with 0.05% (v/v) Tween 20. The seeds were harvested after ripening, and VB6 quantitation was performed.

A bacterial growth assay was performed in rice plants at 14 days after inoculation. Ten-centimeter-long leaves from six independent plants

were harvested, surface sterilized in a 70% ethanol solution for 1 min, and then rinsed in sterile distilled water three times. The samples were ground in 2 ml of sterile distilled water followed by serial dilution (1:10) and plating on NA medium containing 50 $\mu\text{g ml}^{-1}$ rifampicin at 28°C for colony counting. The experiment was repeated three times. The means were compared using Student's *t*-test. The standard error and *t*-test results were recorded.

Stomatal aperture measurement

The stomatal apertures on the leaves of rice or *Arabidopsis* plants were measured as reported by Melotto et al. (2006). Rice or *Arabidopsis* plants were kept under light for at least 3 h and then treated with VB6 or ABA or inoculated with *Xoc* strains. Leaves were harvested at 1 and 8 h after treatment. The stomatal apertures were measured using an LSM 880 NLO confocal microscope (Zeiss).

RNA extraction, reverse transcription-polymerase chain reaction, and quantitative real-time PCR

Leaves or whole plants were collected to extract total RNA using the TRIzol Reagent (Invitrogen). RevertTra Ace qPCR RT Master Mix with gDNA Remover (TOYOBO) and 1 μg of total RNA were used to synthesize first-strand cDNA according to the manufacturer's instructions. Quantitative real-time PCR was performed with a QuantStudio 6 Flex Real-Time PCR System (Life Technologies) using KOD SYBR qPCR Mix (TOYOBO) as described in the manufacturer's instructions. The primers used for quantitative real-time PCR are described in Supplemental Table 2.

Protein interaction analysis

Y2H assays were used to screen protein interactions with the Matchmaker Gold Yeast Two-Hybrid System (Clontech) as described in the manufacturer's instructions. In brief, the plasmids pGBKT7-avrRxo1(109–421) and pGADT7-OsPDX1.2 were transformed into Y2H Gold yeast cells, which were then grown on double dropout medium (SD-Leu/-Trp) and quadruple dropout medium (SD-His/-Leu/-Trp/-Ura).

BiFC was used to examine the protein interactions as described previously (Walter et al., 2004). In brief, *Agrobacterium* GV3101 cells containing the AvrRxo1-MYC-nYFP and OsPDX1.2-HA-cYFP plasmids were resuspended in agroinfiltration buffer (10 mM MgCl₂, 10 mM 2-(N-morpholino) ethanesulfonic acid [MES], pH 5.6, 200 mM acetosyringone), and the optical density at 600 nm was adjusted to 1.0. These suspensions were mixed in equal amounts and infiltrated into 4-week-old *N. benthamiana* leaves with a needleless syringe. Three days later, the leaves were observed using an LSM 880 NLO confocal microscope (Zeiss).

A coIP assay was performed to examine protein interactions as described previously (Moffett et al., 2002). In brief, the agroinfiltrated tobacco leaves were harvested and ground to a fine powder in liquid nitrogen, and the powder was resuspended in protein extraction buffer (50 mM Tris-HCl [pH 7.5], 150 mM NaCl, 50 mM glucose, 0.1% Triton X-100, 0.5 mM dithiothreitol, 10 mM NaF, 1 mM Na₃VO₄, 25 mM β -sodium glycerophosphate, 1 mM PMSF, and 1 \times protease inhibitor cocktail [Sigma]) for 1 h. MYC-Trap beads were used to immunoprecipitate the proteins, and the eluted proteins were further analyzed by SDS-PAGE and western blotting. An anti-OsPDX1 antibody raised against DDAHINKHN epitope peptides was produced by Abmart and used at a 1:1000 dilution. The anti-c-Myc tag antibody was used against c-Myc-tagged protein (1:3000; Abmart). The secondary antibody used was horseradish-peroxidase-conjugated goat anti-mouse immunoglobulin G (Sigma; 1:10 000).

Protein purification and degradation analyses

The MBP-AvrRxo1-6 \times His and OsPDX1.2-6 \times His proteins were purified by Ni²⁺ affinity chromatography using cComplete His-Tag Purification Resin (Roche). Protein concentrations were measured with a NanoDrop spectrophotometer and via SDS-PAGE. The purified MBP-AvrRxo1-6 \times His protein (1 μg) and OsPDX1.2-6 \times His proteins (5 μg) were mixed in reaction

buffer (25 mM Tris-HCl [pH 7.5], 10 mM MgCl₂, 10 mM NaCl, 10 mM ATP) and incubated at 37°C for 2 h. The interaction products were further analyzed by SDS-PAGE and western blotting.

Quantitation of VB6

VB6 was extracted and quantitated as described previously (Wagner et al., 2006). In brief, leaves from 4-week-old rice plants and ripe seeds were powdered in liquid nitrogen, suspended in 0.1 M HCl, and boiled for 30 min at 120°C. The extracts were treated with acid phosphatase (Sigma-Aldrich) and β -glucosidase (Sigma-Aldrich). The contents of pyridoxine, pyridoxal, and pyridoxamine were determined via HPLC using solvents A (0.1% acetic acid) and B (acetonitrile). Pyridoxine-hydrochloride, pyridoxal-hydrochloride, and PM dihydrochloride (Sigma-Aldrich) served as standards.

Quantitation of ABA levels

The leaves of 4-week-old seedlings were used for ABA quantification. To examine the effects of *Xoc* invasion on the level of ABA, rice seedlings were dip inoculated with RS105, RS105 Δa (*avrRxo1* KO mutant), or RS105 Δa -CP (the complementary strain). To examine the effects of VB6 on the level of ABA, leaves of 4-week-old seedlings were treated with VB6 (100 μM) or ddH₂O by injection. Samples of 100 mg each were prepared and quantified using an HPLC-MS/MS system as reported previously (Xu et al., 2016). At least three biological replicates were analyzed. ABA was also detected using immunocytochemistry in the leaves of rice and *Arabidopsis* as reported elsewhere (Ondzighi-Assoume et al., 2016). In brief, the leaves were soaked in buffer, vacuum infiltrated at 4°C, and then incubated at 4°C overnight with shaking. Thereafter, the samples were hyalinized and incubated with an anti-ABA polyclonal antibody (Invitrogen). Next, the samples were incubated with a goat anti-rabbit immunoglobulin G secondary antibody (Invitrogen). The resulting fluorescence signals were measured using an LSM 880 NLO confocal microscope (Zeiss).

Aldehyde oxidase activity assay

Aldehyde oxidase activity was analyzed as reported previously (Seo et al., 2000a). Rice leaves were ground to a powder in liquid nitrogen and suspended in extraction buffer (50 mM Tris HCl [pH 7.5], 1 mM EDTA, 1 μM sodium molybdate, 10 μM flavin adenine dinucleotide, 2 mM dithiothreitol) to extract total proteins, which were then subjected to native PAGE. The bands corresponding to abscisic aldehyde activity were developed with abscisic aldehyde (Sigma-Aldrich) at 30°C in the dark for 30 min.

SUPPLEMENTAL INFORMATION

Supplemental information can be found online at *Plant Communications Online*.

FUNDING

This study was supported by the National Natural Science Foundation (31872925 and 32072500), Natural Science Outstanding Youth Fund of Shandong Province (JQ201807), Shandong Province Key Research and Development Plan (2019JZZY020608, 2020CXGC010803, and 2019GN C106152), Science and Technology Support Plan for Youth Innovation of Colleges and Universities of Shandong Province (2019KJF023), and the National Key Research and Development Program of China (2016YFD0100903). X.D. thanks S.H. for hosting his research visit at Michigan State University, supported by the United States National Institute of General Medical Sciences (GM109928).

AUTHOR CONTRIBUTIONS

X.D., H.L., and Z.C. conceived and designed the experiments. H.L., C.L., T.W., B.Z., B.L., Q.X., and W.F. performed the experiments. H.L., S.H., Y.L., and X.D. analyzed the data. H.L., S.H., and X.D. wrote the manuscript, and H.D. helped with revisions.

ACKNOWLEDGMENTS

We are grateful to Professor Lizhong Xiong (Huazhong Agricultural University) for providing the *bzip23* mutant and Professor Jun Fang (Northeast Institute of Geography and Agroecology, CAS) for providing the *osaba1* mutant. No conflict of interest is declared.

Received: November 28, 2021

Revised: March 15, 2022

Accepted: April 8, 2022

Published: May 9, 2022

REFERENCES

- Bittner, F., Oreb, M., and Mendel, R.R.** (2001). ABA3 is a molybdenum cofactor sulfuryase required for activation of aldehyde oxidase and xanthine dehydrogenase in *Arabidopsis thaliana*. *J. Biol. Chem.* **276**:40381–40384.
- Chen, L., Qu, X., Hou, B., Sosso, D., Osorio, S., Fernie, A.R., and Frommer, W.B.** (2012). Sucrose efflux mediated by SWEET proteins as a key step for phloem transport. *Science* **335**:207–211.
- Chen, S., Songkumarn, P., Liu, J., and Wang, G.L.** (2009). A versatile zero background T-vector system for gene cloning and functional genomics. *Plant Physiol.* **150**:1111–1121.
- Chen, W., Gao, Y., Xie, W., Gong, L., Lu, K., Wang, W., Li, Y., Liu, X., Zhang, H., Dong, H., et al.** (2014). Genome-wide association analyses provide genetic and biochemical insights into natural variation in rice metabolism. *Nat. Genet.* **46**:714–721.
- Clough, S.J., and Bent, A.F.** (1998). Floral dip: a simplified method for *Agrobacterium*-mediated transformation of *Arabidopsis thaliana*. *Plant J.* **16**:735–743.
- Colinas, M., Eisenhut, M., Tohge, T., Pesquera, M., Fernie, A.R., Weber, A.P., and Fitzpatrick, T.B.** (2016). Balancing of B6 vitamers is essential for plant development and metabolism in *Arabidopsis*. *Plant Cell* **28**:439–453.
- Denslow, S.A., Rueschhoff, E.E., and Daub, M.E.** (2007). Regulation of the *Arabidopsis thaliana* vitamin B (6) biosynthesis genes by abiotic stress. *Plant Physiol. Biochem.* **45**:152–161.
- Denslow, S.A., Walls, A.A., and Daub, M.E.** (2005). Regulation of biosynthetic genes and antioxidant properties of vitamin B6 vitamers during plant defense responses. *Physiol. Mol. Plant Pathol.* **66**:244–255.
- Du, M., Zhai, Q., Deng, L., Li, S., Li, H., Yan, L., Huang, Z., Wang, B., Jiang, H., Huang, T., et al.** (2014). Closely related NAC transcription factors of tomato differentially regulate stomatal closure and reopening during pathogen attack. *Plant Cell* **26**:3167–3184.
- Gimenez-Ibanez, S., Boter, M., Ortigosa, A., Garcia-Casado, G., Chini, A., Lewsey, M.G., Ecker, J.R., Ntoukakis, V., and Solano, R.** (2017). JAZ2 controls stomata dynamics during bacterial invasion. *New Phytol.* **213**:1378–1392.
- Han, Q., Zhou, C., Wu, S., Liu, Y., Triplett, L., Miao, J., Tokuhisa, J., Deblais, L., Robinson, H., Leach, J.E., et al.** (2015). Crystal structure of *Xanthomonas* AvrRxo1-ORF1, a type III effector with a polynucleotide kinase domain, and its interactor AvrRxo1-ORF2. *Structure* **23**:1900–1909.
- Hong, Y., Wang, Z., Shi, H., Yao, J., Liu, X., Wang, F., Zeng, L., Xie, Z., and Zhu, J.K.** (2020). Reciprocal regulation between nicotinamide adenine dinucleotide metabolism and abscisic acid and stress response pathways in *Arabidopsis*. *PLoS Genet.* **16**:e1008892.
- Issak, M., Okuma, E., Munemasa, S., Nakamura, Y., Mori, I.C., and Murata, Y.** (2013). Neither endogenous abscisic acid nor endogenous jasmonate is involved in salicylic acid-, yeast elicitor-, or chitosan-induced stomatal closure in *Arabidopsis thaliana*. *Biosci. Biotechnol. Biochem.* **77**:1111–1113.
- Leung, J., Bouvier-Durand, M., Morris, P.C., Guerrier, D., Chedford, F., and Giraudat, J.** (1994). *Arabidopsis* ABA response gene AB11: features of a calcium-modulated protein phosphatase. *Science* **264**:1448–1452.
- Liao, Y., Bai, Q., Xu, P., Wu, T., Guo, D., Peng, Y., Zhang, H., Deng, X., Chen, X., Luo, M., et al.** (2018). Mutation in rice Abscisic Acid2 results in cell death, enhanced disease-resistance, altered seed dormancy and development. *Front. Plant Sci.* **9**:405.
- Lievens, L., Pollier, J., Goossens, A., et al.** (2017). Abscisic acid as pathogen effector and immune regulator. *Front. Plant Sci.* **8**:587.
- Lim, C.W., and Lee, S.C.** (2015). *Arabidopsis* abscisic acid receptors play an important role in disease resistance. *Plant Mol. Biol.* **88**:313–324.
- Lin, Y.J., and Zhang, Q.F.** (2005). Optimising the tissue culture conditions for high efficiency transformation of *indica* rice. *Plant Cell Rep.* **23**:540–547.
- Liu, H., Chang, Q., Feng, W., Zhang, B., Wu, T., Li, N., Yao, F., Ding, X., and Chu, Z.** (2014). Domain dissection of *avrRxo1* for suppressor, avirulence and cytotoxicity functions. *PLoS One* **9**:e113875.
- Ma, X., Zhu, Q., Chen, Y., and Liu, Y.G.** (2016). CRISPR/Cas9 platforms for genome editing in plants: developments and applications. *Mol. Plant.* **9**:961–974.
- Melotto, M., Underwood, W., Koczan, J., Nomura, K., and He, S.Y.** (2006). Plant stomata function in innate immunity against bacterial invasion. *Cell* **126**:969–980.
- Melotto, M., Zhang, L., Oblessuc, P.R., and He, S.Y.** (2017). Stomatal defense a decade later. *Plant Physiol.* **174**:561–571.
- Moffett, P., Farnham, G., Peart, J., and Baulcombe, D.C.** (2002). Interaction between domains of a plant NBS-LRR protein in disease resistance-related cell death. *EMBO J.* **21**:4511–4519.
- Montillet, J., Leonhardt, N., Mondy, S., Tranchimand, S., Rumeau, D., Boudsocq, M., Garcia, A.V., Douki, T., Bigeard, J., Laurière, C., et al.** (2013). An abscisic acid-independent oxylipin pathway controls stomatal closure and immune defense in *Arabidopsis*. *Plos Biol.* **11**:e1001513.
- Mooney, S., Leuendorf, J., Hendrickson, C., and Hellmann, H.** (2009). Vitamin B6: a long known compound of surprising complexity. *Molecules* **14**:329–351.
- Murray, R.R., Emblow, M.S.M., Hetherington, A.M., and Foster, G.D.** (2016). Plant virus infections control stomatal development. *Sci. Rep.* **6**:34507.
- Nino-Liu, D., Ronald, P., and Bogdanove, A.J.** (2006). *Xanthomonas oryzae* pathovars: model pathogens of a model crop. *Mol. Plant Pathol.* **7**:303–324.
- Ondzighi-Assoume, C.A., Chakraborty, S., and Harris, J.M.** (2016). Environmental nitrate stimulates abscisic acid accumulation in *Arabidopsis* root tips by releasing it from inactive stores. *Plant Cell* **28**:729–745.
- Schellenberg, B., Ramel, C., and Dudler, R.** (2010). *Pseudomonas syringae* virulence factor syringolin A counteracts stomatal immunity by proteasome inhibition. *Mol. Plant Microbe Interact.* **23**:1287–1293.
- Schuebel, F., Rucker, A., Edelman, D., Schessner, J., Brieke, C., and Meinhart, A.** (2016). 3'-NADP and 3'-NAADP, two metabolites formed by the bacterial type III effector AvrRxo1. *J. Biol. Chem.* **291**:22868–22880.
- Schwartz, S.H., Léon-Kloosterziel, K.M., Koornneef, M., and Zeevaart, J.A.** (1997). Biochemical characterization of the *aba2* and *aba3* mutants in *Arabidopsis thaliana*. *Plant Physiol.* **114**:161–166.
- Seo, M., Koiwai, H., Akaba, S., Komano, T., Oritani, T., Kamiya, Y., and Koshiba, T.** (2000a). Abscisic aldehyde oxidase in leaves of *Arabidopsis thaliana*. *Plant J.* **23**:481–488.

- Seo, M., Peeters, A.J., Koiwai, H., Oritani, T., Marion-Poll, A., Zeevaert, J.A., Koornneef, M., Kamiya, Y., and Koshiba, T. (2000b). The *Arabidopsis* aldehyde oxidase 3 (AO3) gene product catalyzes the final step in abscisic acid biosynthesis in leaves. *Proc. Natl. Acad. Sci. USA* **97**:12908–12913.
- Shidore, T., Broeckling, C.D., Kirkwood, J.S., Long, J.J., Miao, J., Zhao, B., Leach, J.E., and Triplett, L.R. (2017). The effector AvrRxo1 phosphorylates NAD in planta. *PLoS pathog.* **13**:e1006442.
- Su, J., Zhang, M., Zhang, L., Sun, T., Liu, Y., Lukowitz, W., Xu, J., and Zhang, S. (2017). Regulation of stomatal immunity by interdependent functions of a pathogen-responsive MPK3/MPK6 cascade and abscisic acid. *The Plant Cell* **29**:526–542.
- Thor, K., Jiang, S., Michard, E., George, J., Scherzer, S., Huang, S., Dindas, J., Derbyshire, P., Leitão, N., DeFalco, T.A., et al. (2020). The calcium-permeable channel OSCA1.3 regulates plant stomatal immunity. *Nature* **585**:569–573.
- Titiz, O., Tambasco-Studart, M., Warzych, E., Apel, K., Amrhein, N., Laloi, C., and Fitzpatrick, T.B. (2006). Pdx1 is essential for vitamin B6 biosynthesis, development and stress tolerance in *Arabidopsis*. *Plant J.* **48**:933–946.
- Triplett, L.R., Shidore, T., Long, J., Miao, J., Wu, S., Han, Q., Zhou, C., Ishihara, H., Li, J., Zhao, B., et al. (2016). AvrRxo1 is a bifunctional type III secreted effector and toxin-antitoxin system component with homologs in diverse environmental contexts. *PLoS One* **11**:e0158856.
- Wagner, S., Bernhardt, A., Leuendorf, J.E., Drewke, C., Lytovchenko, A., Mujahed, N., Gurgui, C., Frommer, W.B., Leistner, E., Fernie, A.R., et al. (2006). Analysis of the *Arabidopsis* *rsr4-1/pdx1-3* mutant reveals the critical function of the PDX1 protein family in metabolism, development, and VB6 biosynthesis. *Plant Cell* **18**:1722–1735.
- Walter, M., Chaban, C., Schütze, K., Batistic, O., Weckermann, K., Näke, C., Blazevic, D., Grefen, C., Schumacher, K., Oecking, C., et al. (2004). Visualization of protein interactions in living plant cells using bimolecular fluorescence complementation. *Plant J.* **40**:428–438.
- Wang, S., Li, S., Wang, J., Li, Q., Xin, X.F., Zhou, S., Wang, Y., Li, D., Xu, J., Luo, Z.Q., et al. (2021). A bacterial kinase phosphorylates OSK1 to suppress stomatal immunity in rice. *Nat. Commun.* **12**:5479.
- Xiang, Y., Tang, N., Du, H., Ye, H.Y., and Xiong, L.Z. (2008). Characterization of OsbZIP23 as a key player of the basic leucine zipper transcription factor family for conferring abscisic acid sensitivity and salinity and drought tolerance in rice. *Plant Physiol.* **148**:1938–1952.
- Xin, X.F., and He, S.Y. (2013). *Pseudomonas syringae* pv. *tomato* DC3000: a model pathogen for probing disease susceptibility and hormone signaling in plants. *Annu. Rev. Phytopathol.* **51**:473–498.
- Xu, Q., Truong, T.T., Barrero, J.M., Jacobsen, J.V., Hocart, C.H., and Gubler, F. (2016). A role for jasmonates in the release of dormancy by cold stratification in wheat. *J. Exp. Bot.* **67**:3497–3508.
- Yang, B., Sugio, A., and White, F.F. (2006). *Os8N3* is a host disease-susceptibility gene for bacterial blight of rice. *Proc. Natl. Acad. Sci. USA* **103**:10503–10508.
- Zhang, D., Tian, C., Yin, K., Wang, W., and Qiu, J.L. (2019). Postinvasive bacterial resistance conferred by open stomata in rice. *Mol. Plant-microb. Interact.* **32**:255–266.
- Zhang, Y., Jin, X., Ouyang, Z., Li, X., Liu, B., Huang, L., Hong, Y., Zhang, H., Song, F., and Li, D. (2015). Vitamin B6 contributes to disease resistance against *Pseudomonas syringae* pv. *tomato* DC3000 and *Botrytis cinerea* in *Arabidopsis thaliana*. *Plant Physiol.* **175**:21–25.
- Zhang, Y., Liu, B., Li, X., Ouyang, Z., Huang, L., Hong, Y., Zhang, H., Li, D., and Song, F. (2014). The de novo biosynthesis of vitamin B6 is required for disease resistance against *Botrytis cinerea* in tomato. *Mol. Plant Microbe Interact.* **27**:688–699.
- Zhao, B., Ardales, E.Y., Raymundo, A., Bai, J., Trick, H.N., Leach, J.E., and Hulbert, S.H. (2004). The *avrRxo1* gene from the rice pathogen *Xanthomonas oryzae* pv. *oryzicola* confers a nonhost defense reaction on maize with resistance gene *Rxo1*. *Mol. Plant Microbe Interact.* **17**:771–779.
- Zhao, B., Lin, X., Poland, J., Trick, H., and Hulbert, S. (2005). A maize resistance gene functions against bacterial streak disease in rice. *Proc. Natl. Acad. Sci. USA* **102**:15383–15388.
- Zheng, X.Y., Zhou, M., Yoo, H., Pruneda-Paz, J.L., Spivey, N.W., Kay, S.A., and Dong, X. (2015). Spatial and temporal regulation of biosynthesis of the plant immune signal salicylic acid. *Proc. Natl. Acad. Sci. USA* **112**:9166–9173.